Single particle characterization and total elemental concentration measurements in polar ice using CFA-icpTOF

Tobias Erhardt,*,† Camilla M. Jensen,† Olga Borovinskaya,‡ and Hubertus Fischer†

†*Climate and Environmental Physics and Oeschger Center for Climate Change Research, University of Bern, Sidlerstrasse 5, 3012 Bern, Switzerland*

‡*TOFWERK, Uttigenstrasse 22, CH-3600 Thun, Switzerland*

E-mail: erhardt@climate.unibe.ch

Abstract

Continuous flow analysis (CFA) has become widely used for the measurement of aerosol-derived impurities in ice core samples resulting in high-resolution data sets of past aerosol deposition. Here we present first results from coupling an inductively coupled plasma time-of-flight mass spectrometer (ICP-TOFMS) to a traditional CFA system. This setup enables the measurement of exactly co-registered elemental concentrations over the full mass range without degradation of sensitivity with increasing number of analytes. The resulting total elemental concentration records have similar or better resolution than the established spectrophotometric methods. The unique capability of a TOFMS to measure fast transient signals and to still cover the full mass range furthermore enables the detection of the ionization of individual insoluble particles entering the plasma. The resulting mass spectra of the particles can be used to

investigate the relative elemental composition of the mineral dust particles preserved in the ice. The presented analysis of iron-bearing particles indicates that most of the particulate iron in the Greenland ice is associated with Mg and Al and is likely part of clay minerals such as illite.

Introduction

Ice cores as climate archives carry a wealth of information ranging from past atmospheric composition to temperature changes. Among the variables routinely measured in ice-core samples are chemical impurities resulting from the deposition of aerosols on glaciers and ice sheets. The main problem in determining the concentration of aerosol constituents in ice core samples is the risk of contamination and as a result the labor-intensive sample preparation and decontamination. Continuous flow analysis (CFA) overcomes this challenge by continuously melting a vertical cut of the ice core, separating the melt water from the contaminated outer part of the ice stick from the clean inner part. Subsequently, the clean melt water is either collected and measured in discrete aliquots or analyzed continuously.

Concentrations of dissolved ions in the CFA melt water are typically measured using spectrophotometric and fluorimetric techniques specifically optimized for the application to ice core CFA[1–4]. Additionally the concentration and size distribution of insoluble particles are determined using laser light extinction[5]. The continuous determination of the impurities in the melt water yields high depth-resolution and thus time-resolution records that can resolve the seasonal variability of the aerosol deposition on the polar ice sheets. High resolution CFA data from Greenland ice cores have recently been used to investigate episodic aerosol deposition from wild fires throughout the last glacial period[6], the influence of en-route washout by precipitation[7], and small timing differences between rapid climate variability in different parts of the Earth system[8].

Atomic spectroscopy in the form of inductively coupled plasma mass spectroscopy (ICP-MS) coupled to CFA has extended the range of analytes to elemental and trace elemental

concentration in polar and alpine ice[9,10]. These methods have for example enabled the detailed reconstruction of the emission of toxic heavy metals into the atmosphere back in time[11]. Until now, all ICP instruments coupled to continuous flow analysis systems used either quadrupole (QMS) or sector field (SFMS) mass analyzers[9,10]. Of these two methods, SFMS is characterized by higher mass-resolving power and higher sensitivity. The major draw back of both QMS and SFMS mass analyzers is, that they only measure a single mass at any given time. Therefore, to measure the concentrations of multiple elements, these instruments need to sequentially scan through the analyte masses. Especially when considering the rapidly increasing number of masses that need to be monitored to correct for spectral inferences, the sensitivities for the monitored masses will be limited. Depending on the instrument and the number of analytes the mass scanning can take multiple seconds[9]. This fundamentally limits the number of elements that can be measured quasi simultaneously using a single ICP-MS with a sequential mass analyzer.

In recent years sensitive time-of-flight mass analyzers (TOFMS) have become available for ICP ion sources[12]. Due to their operating principle, TOFMS measure all analyte masses at virtually the same time, thus overcoming the instrumental limitations of scanning mass analyzers. Furthermore the fast repetition rate of a TOFMS allows for the multi-elemental detection of fast transient signals resulting for example from the ionization of single particles in the ICP, enabling multi-elemental single particle ICP-MS studies (sp-ICP-MS) e.g.[13]. To leverage this potential for total concentration and single particle analysis in the context of ice-core analysis a commercially available ICP-TOFMS, icpTOF (TOFWERK, Thun Switzerland), has been incorporated into the Bern CFA system[4]. In the following we will first briefly describe the Bern CFA setup, before describing the icpTOF instrument and its coupling into the CFA melt water stream and data acquisition. After that the data treatment for the icpTOF data both for regular, i.e. total concentration, as well as single-particle measurements is described. The results from the icpTOF are then compared to the wet-chemistry CFA data, followed by first results from the single-particle analysis of Fe-bearing

particles in a section of the East Greenland Ice Coring Project (EastGRIP) ice core.

Methods

CFA

In its standard configuration, the Bern CFA system melts ice and firn sticks of 35×35 mm cross section on a gold-plated melt head. The melter unit is situated in a cold (-20 °C) cell inside the Bern CFA warm lab that is also used to prepare the ice samples. The melt head is designed in such a way that the melt water from the outer, possibly contaminated part of the ice stick is separated from the inner, clean part with an area of 26×26 mm[14]. During the melting, an optical encoder records the progress of the melting using a weight sitting on top of the ice stick. For recent measurement campaigns the melter setup has been modified from the original design[4] to allow for reloading of samples during a measurement run to increase sample throughput to around 3 meters per measurement run. In this configuration around 12-14 m of ice can be melted in a 16 h measurement day at average meltspeeds of 2.8 cm min^{-1}, including startup/shutdown and alternating sample/calibrations runs. Melt water from both the inner and the outer part of the melt head is pumped from the cold room to the wet-chemistry analysis system that is described in more detail in[4], to the icpTOF and to other instruments using peristaltic pumps.

CFA-icpTOF

The ICP-TOFMS used in this study is the commercially available icpTOF R produced by TOFWERK AG, Thun, Switzerland. The instrument uses the ICP generation, ion-optics and the collision/reaction cell (Q-Cell) of an iCAP-RQ instrument (Thermo Scientific, Bremen, Germany). In the icpTOF, the original quadrupole mass analyzer of the iCAP-RQ is replaced by a quadrupole notch filter and time-of-flight mass analyzer, both built and integrated by TOFWERK. The quadrupole notch filter[15] is used to attenuate high-intensity spectral peaks

to reduce signal background and to protect the detector of the TOFMS. Evaluation of the icpTOF has shown that it has similar sensitivities as current quadrupole instruments and that it has a linear dynamic range greater than 1 million[16]. Even though the icpTOF records full mass spectra from m/z 7 to 275 at a rate of 33 000 Hz, the usable range of masses and the acquisition speed is limited by the optimization of the ion optics and the maximum possible continuous data transfer rate from the data acquisition hardware to the data acquisition computer. In the presented study, the ion optics were tuned in such a way, that masses below m/z 23 are not transmitted but good sensitivities could be reached across a wide range of analytes present in the ice-core samples. The Q-Cell is pressurized with a mixture of 7 % H_2 in He (Carbagas, Bern, Switzerland) to remove Argide interferences and to thermalize ion energies, leading to improved mass resolution. For example, this enables the measurement of Fe using its most abundant isotope, $^{56}Fe^+$, which is otherwise interfered by ArO^+. The ion optics and TOFMS voltages were optimized to yield maximum sensitivity at a mass resolution of 3000 ($m/\Delta m$, full width at half maximum). In this way interference peaks resulting from impurities in the collision cell gas can be resolved from the analytes without compromising the overall sensitivity. Typical ICP, Q-Cell, notch filter and MS parameters used in this study can be found in Table 1. During measurement campaigns, the plasma conditions are optimized at the beginning of each measurement day. For the continuous measurements, full mass spectra were acquired with two different integration times with a standard 250 ms mode (integrating 8250 spectra), and a selectively applied single-particle mode with 2 ms integration time (integrating 66 spectra). The latter is limited by the rate data can be transferred from the data acquisition system to the connected PC. It is worth noting, that the sensitivity of the icpTOF measurements is not affected by the data acquisition rate as they are achieved by summing a different number of TOF extractions within the data acquisition hardware before transferring the data to the PC.

The icpTOF is directly connected to the melt head of the Bern CFA system and is otherwise kept largely independent from the wet-chemistry CFA system. A mixed air/melt water

stream of 1 ml/min for the icpTOF is split off the melt water stream to the wet chemistry CFA system just downstream of the melt-head using 0.5 mm inner diameter high purity PFA tubing. To limit signal dispersion and efficiently transport particles from the melt head to the icpTOF's sample introduction, the air is removed from the sample stream as late as possible. The air in the segmented flow is contained within the melted ice samples (approximately 10 % by volume) and thus does not present any additional risk of contamination. Removal of the air is achieved using a custom made PTFE low-volume debubbler ($\sim 100\,\mu l$).

Just upstream of the nebulizer, the sample stream is acidified to 1 % HNO_3 using high-purity nitric acid (Optima grade, Fisher Scientific). The sample is then introduced into the plasma using a glass concentric nebulizer (MicroMist, Glass Expansion) and a quartz cyclonic spray chamber cooled to 2 °C. Together with the acid, Rh (TraceCert, Sigma Aldric) is added as an internal standard to the sample stream to monitor the system stability during the multi-hour measurement runs. The acidification of the sample stream serves the main purpose of reducing the washout time from the nebulizer and spray chamber. It is done comparatively late, so that small particles are not dissolved into the matrix. Leaching experiments with dust samples similar to that found in ice cores indicate that within the short exposure time of the sample to the acid, which is in the order of a few seconds, no significant dissolution of particles is expected to occur[17].

Table 1: Instrument parameters used in the presented study

Plasma power	1550 W
Auxiliary gas flow	1 L min^{-1}
Cooling gas flow	14 L min^{-1}
Nebulizer gas flow	1 L min^{-1}
Nebulizer liquid flow	400 µL min^{-1}
Collision gas flow	5.5 mL min^{-1}
Attenuated masses	$^{14}N_2^+$,$^{16}O_2^+$
TOF extractions	33 kHz
Integration time (standard)	250 ms
Integration time (single particle)	2 ms

Calibration

During routine measurements, calibration measurements are performed approximately every two hours, bracketing each measurement run. Calibration stock dilutions are made by mixing multiple multi-element standards (TraceCert, Sigma Aldrich) which are further diluted into working standards that span the range of observed concentrations in the ice every week. All dilutions were performed gravimetrically in acid-cleaned FEP and HDPE containers using high-purity nitric acid and ultra high purity water. The standard solutions are introduced by flow-injection from a sample loop into a 1 % HNO_3 carrier stream. Table 2 shows the averages of the sensitivities, their uncertainties given as relative standard deviation (RSTD), background equivalent concentrations (BEC) and limits of detection (LOD) for the analytes discussed in this paper. LODs are calculated using three times the standard deviation of the blanks and for the final dataset at 1 mm depth resolution assuming an average melt speed of 2.8 cm min^{-1}.

To relate the number of detected particle events in the sp-ICP-MS data to the number concentration in the melt water stream, the transport efficiency of the sample introduction system needs to be determined. This was done using 60 nm gold nanoparticles (Nanocomposix, San Diego, USA) using the particle counting method[18], resulting in a transport efficiency of (8.6±0.3) % (1σ). Results from the direct nebulisation of slurries indicate that particles smaller diameters than 2 µm are transported efficiently through the spray chamber and that below that size the influence of particle size on transport efficiency is negligible[19,20]. Because the vast majority of the mineral dust particles found in Greenland ice are smaller than this size cutoff[5], the transport efficiency determined using the nanoparticles can be applied to the data presented here.

icpTOF data processing

The raw mass spectrum data from the icpTOF is processed using TofWare (Tofwerk, Thun). To account for slight changes in the time-of-flight to mass relationship during the course of

Table 2: Typical calibration results for the elements discussed here. All values are averages from the calibration measurements performed during a measurement campaign, totaling 128 measurements over 6 weeks. LODs were calculated for both 1 s and 1 mm resolution data, assuming a melt speed of 2.8 cm min^{-1}. Note that the sensitivities here are long-term averages and differ from calibration to calibration.

Element	Ion	Sensitivity (cps/ppb)	RSTD (%)	BEC (ppt)	1 s LOD (ppt)	1 mm LOD (ppt)
Na	$^{23}Na^{+}$	319.2	4.9	644.4	134.1	91.6
Mg	$^{24}Mg^{+}$	296.3	3.6	95.2	48.3	33.0
Al	$^{27}Al^{+}$	432.5	6.5	695.1	143.5	98.0
Ca	$^{44}Ca^{+}$	66.9	4.1	549.0	245.2	167.5
Fe	$^{56}Fe^{+}$	5950.2	6.3	592.3	109.5	74.8

the measurements, the mass calibration is continuously adjusted using 60 s averages of the raw data. For each time step, mass calibration functions are calculated using ever present peaks in the mass spectra coming from the internal standard, gas impurities in the plasma Ar supply, or background contamination. Following the mass calibration, the peaks of all analyte ions are integrated after the removal of the spectral baseline. The resulting intensity time traces are then processed using custom Python scripts to calibrate the data and correct for spectral interferences. The finished concentration time series are subsequently aligned to the wet-chemistry CFA data and through that to the ice-core depth scale. This is achieved by automatically matching the ICP total Ca concentration and wet-chemistry dissolved Ca^{2+} time traces. In a final step, data for the elemental concentrations are filtered with a 10 s Gaussian filter to remove variability beyond the limit of the sample introduction system and are then downsampled to 1 mm nominal depth resolution to match the nominal resolution of the wet-chemistry CFA data. In this step, data around ice-core breaks are masked out to remove signals from contamination. The high-resolution mass-spectrum data intended for the single-particle analysis is treated identically to obtain a complete and homogeneous 1 mm resolution dataset for all measured ice samples. Note, that the LODs presented in Table 2 do not take into account the additional reduction of the background standard deviation due to the smoothing, which would further reduce the LODs.

To identify particle signals in the high-resolution data a custom algorithm is applied to the high-resolution time traces of individual analyte ions. The algorithm is derived from the commonly used thresholding approach based on the average background signal intensity and its standard deviation. Differing from measurements of discrete samples, the background concentrations in the melt water stream continuously changes with time throughout each measurement. To account for these changes, the average background signal intensity (μ_{bg}) and its standard deviation (σ_{bg}) is calculated using a Gaussian weighted window with cutoff frequency of 10 s. The standard deviation of the background signal intensity is explicitly calculated, instead of assuming a perfect Poisson distribution of the background signal (i.e. $\sigma_{\mathrm{bg}}^2 = \mu_{\mathrm{bg}}$). In this way, the algorithm accounts for the over-dispersion of the background signal due to the data acquisition of the icpTOF[21]. Because of the long measurement times and relative rarity of particle ionization events, it is important to keep the false positive rate of the particle detection algorithm low. In the present study it was set to a theoretical 0.01 % by only considering signals above $\mu_{\mathrm{bg}} + 3.71\,\sigma_{\mathrm{bg}}$ as signals from ionized particles. The false positive rate also dictates the detection of particles in blank solutions to be by definition at least 0.01 % of the observations. For the presented data at 2 ms resolution this translates to a blank counting rate of 0.05 particles per second. The detection threshold is iteratively applied and re-calculated, removing particle signals until a stable solution is reached, typically within 10-20 iterations for a 2 h dataset. To reduce the computational burden of the combination of an iterative approach and the large amounts of data, the algorithm is implemented using Fast Fourier Transformation based convolutions. The algorithm decomposes the signal into two components: the smoothly varying signal off the dissolved background and the net intensity of the peaks above this background resulting from the particle ionizations. Figure 1 shows two seconds of data for $^{56}Fe^{+}$ with the applied threshold and the calculated background intensity from the dissolved part of the signal. After the identification of the particle signals, background signal intensity, net particle intensity above the dissolved background and the number of particles detected in each 1 s interval are downsampled to the nominal 1 mm depth

207 resolution also used in the other data sets.

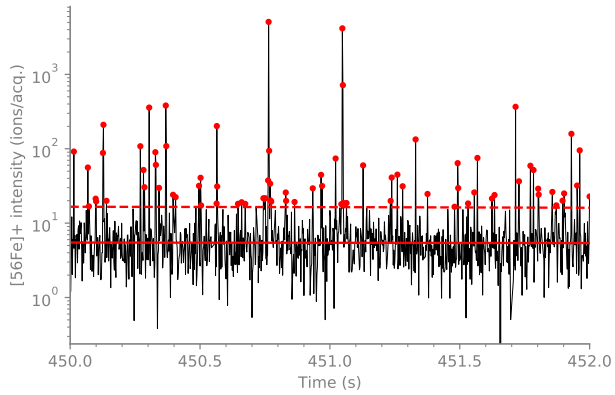

Figure 1: Example of the detection of single particle signals in two seconds of $^{56}Fe^{+}$ data. The solid line shows the inferred dissolved background, the dashed line the threshold over which a signal is defined to be from an ionized particle. Particle signals are marked with red dots. Note, the near lack of negative outliers in the trace strongly supports the assumption, that the positive ones are produced by particle ionizations.

208 Because the background signal continuously changes and its standard deviation is de-
209 pendent on the intensity, the detection limit of particle events in terms of the net-particle
210 intensity above the background continuously changes as well. In practice that means that
211 when the background concentrations in a given element are higher, smaller particles cannot
212 be detected anymore, leading to spurious signals in the determined particle number concen-
213 trations. To circumvent this problem, only particle events larger than the overall highest
214 detection limit in terms of net-peak size in the run are considered for the calculation of the
215 particle number concentration. This is illustrated in Figure 2. It shows iron data spanning
216 multiple annual maxima alongside the inferred dissolved concentration and the variable de-
217 tection limit for particle ionization events. Panel (c) of Figure 2 shows particle detection
218 rates resulting from the variable threshold alongside that from a constant threshold. Only
219 the number of particles detected per second with the constant threshold resembles the signal
220 of the total iron and correlates strongly with the micro-particle concentration shown in the
221 lower most panel of Figure 2.

222 To interpret the data, the background intensities are nominally converted to concentra-

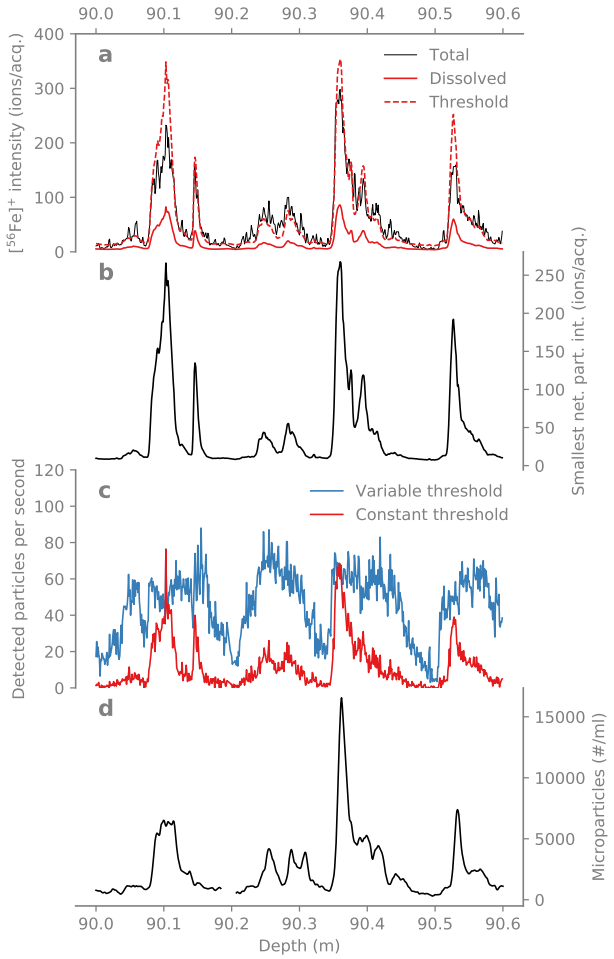

Figure 2: Example for the effect of the variable background concentration on the inferred particle number concentration. The top panel (a) shows the total signal intensity (smoothed with 10 s Gaussian), the inferred dissolved background concentration and the detection threshold for particle ionization events over a 60 cm range of data containing multiple seasonal cycles. Note, that the traces shown in the figure are smoothed and downsampled to 1 mm nominal resolution, whereas the calculations for the particle threshold are based on the much more variable full-resolution data. The resulting smallest net particle intensity that can be detected above the threshold is shown in panel (b). Panel (c) shows the inferred particle concentration using the variable detection threshold and a constant threshold. For comparison, the bottom panel (d), shows the micro particle (particle diameter larger than 1 µm) concentration over the same depth range as measured by an optical particle counter.

tions using the sensitivities obtained from the dissolved standard measurements. Conversion of the net-particle signals to particle masses or sizes is not attempted due to the complex structure and multi-elemental composition of the mineral particles in the ice. The composition of the detected particles is only assessed in terms of elemental ratios, correcting for the different elemental sensitivities determined by the standard measurements. An absolute quantification of the total elemental amounts in the particles would require a particle standard with the same size distribution and mineralogical composition as the dust particles in the ice, which is not available yet.

One important prerequisite for the interpretation of the elemental composition of the detected particles is that each detected event only results from the ionization of a single particle. The probability of detection a signal of more than one particle per observation (i.e. per sample interval) can readily be calculated using Poisson statistics from the fraction of observations that are not identified as particles p_{bg} as:

$$P(n > 1) = 1 - P(n \leq 1) = 1 - (p_{bg}\,(1 - \ln p_{bg}))$$

For the particle concentration results presented here, the coincidence probability for 10^3 particles per ml is $0.3 \cdot 10^{-6}$, and $0.3 \cdot 10^{-3}$ for $100 \cdot 10^3$ particles per ml.

The uncertainty of the net intensity of the particle ionisation signals is governed by the uncertainty of the subtracted background amplitude. That means that especially for small particle signals close to the detection threshold the relative uncertainty can in theory be quite large. However in practice the particle signals are typically much larger than the background, leading to average relative uncertainties between 2.7 % to 12.7 % for Fe and Mg respectively. For the determination of elemental mass ratios, the uncertainties of the respective sensitivities contribute significantly to the overall uncertainty yielding around 15 % RSTD on average for the elemental ratios investigated here.

Results and Discussion

Because the CFA-icpTOF is used for both the measurements of total elemental concentration in the standard CFA mode as well as for single-particle detection in the high-resolution mode, the following section is split up between these two applications. The first part focuses on the comparison of the icpTOF to the established spectrophotometric detection methods for sodium and calcium. The second part deals with the single-particle data and their interpretation both for single- as well as multi-elemental data, focusing on Fe-bearing particles.

Comparison to established CFA detection methods

To characterize the performance of the coupling of the icpTOF to the continuous melting device and the sample introduction system, we compare the CFA-icpTOF data to the wet-chemistry CFA data. In the wet-chemistry CFA setup, concentrations of Na^+ and Ca^+ are determined by well-established spectrophotometric methods. Na^+ concentrations are determined using absorption spectroscopy, Ca^+ concentrations using a fluorimetric method, both optimized for the application in a continuous flow setup[2–4]. Both of these impurities, albeit as elemental concentrations, can also be measured with the icpTOF. Figure 3 shows a three meter section of data from the two spectrophotometric methods alongside their respective counterparts from the icpTOF.

The measurements shown in Figure 3 are individually and independently calibrated using different reference solutions. The Ca^{2+} and Na^+ data are synchronized using multi-ion standard peaks, as described in Kaufmann et al.[4]. The ICP Ca data is aligned to the Ca^{2+} data as described above. Overall, the agreement between the wet chemistry methods and the CFA-icpTOF data is very good especially in the light of the different detection methods and independent calibrations. Nevertheless, there are small systematic difference between the wet-chemistry and the icpTOF data, mainly visible in the higher, sharper peaks in the CFA-icpTOF data and the often lower minima. To quantify the resolution in terms of the

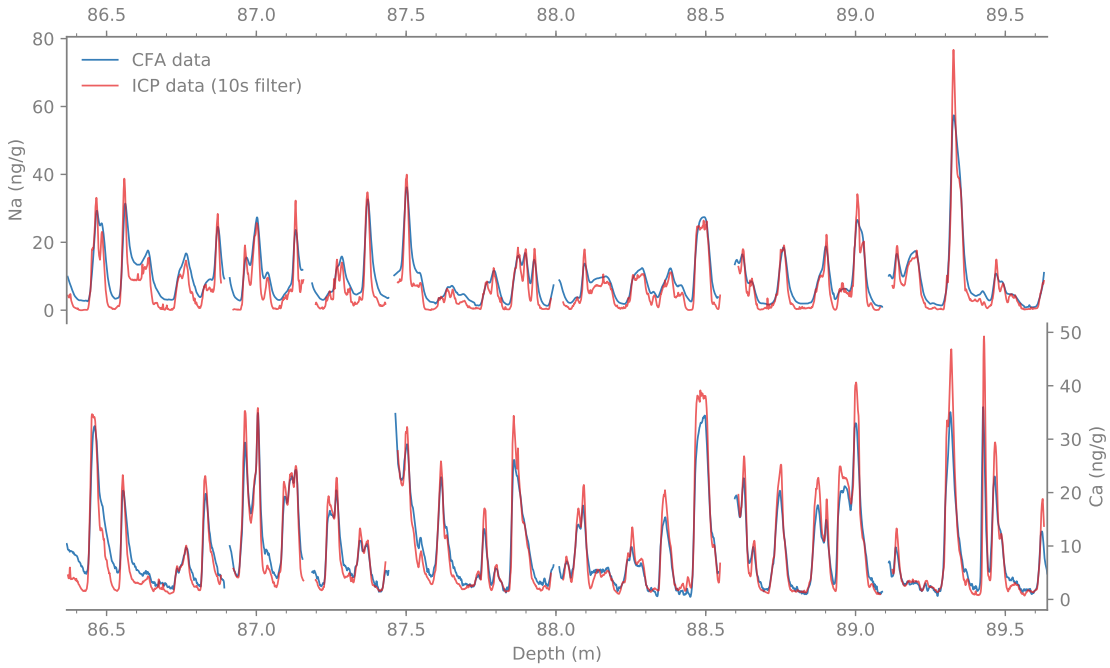

Figure 3: Comparison between wet-chemistry CFA measurements of Na^+ and Ca^{2+} with the Na and Ca concentrations measured by the CFA-icpTOF. Both wet-chemistry methods[4] are completely independent from the CFA-icpTOF in terms of calibrations. The depth scale of the CFA-icpTOF data is transferred from the wet-chemistry Ca^{2+} measurements by aligning their acquisition times. Note that the CFA-icpTOF shows less tailing and lower minima between the annual layer peaks in both Ca and Na as compared to the traditional methods, indicating a slightly higher analytical resolution. The correlation coefficient between the respective methods is 0.96 for both Na and Ca, the RMS differences are 3.35 ppb for Na and 2.64 ppb for Ca respectively.

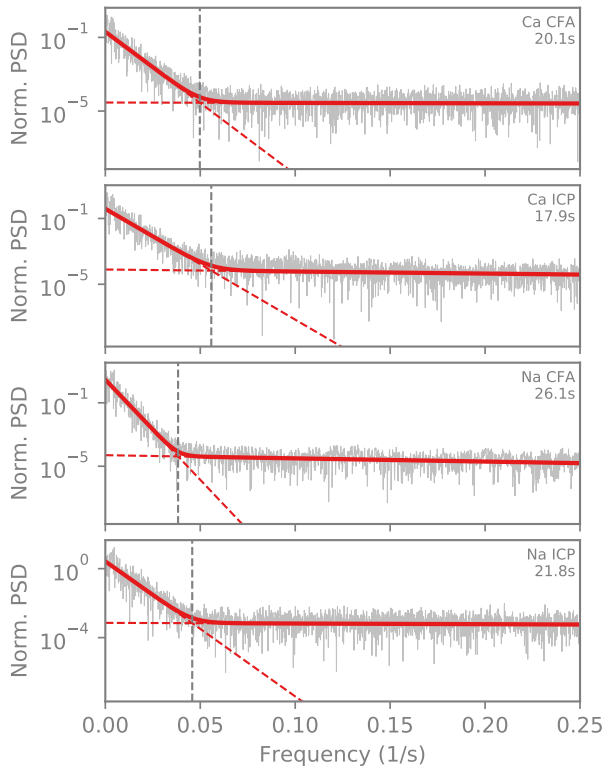

Figure 4: Normalized power spectral densities (PSD) and critical frequencies for the raw, unfiltered data shown in Figure 3. The critical frequencies, at which the noise dominates the signal was determined as the intersection of a bilinear fit to log-power spectral density. The wavelengths indicated by the vertical dashed lines in the figure correspond to 9.4, 8.4, 12.2 and 10.2 mm (from top to bottom) at a 2.8 cm min^{-1} melt rate as used for this measurement run. Overall, the CFA-icpTOF data has significantly higher resolution than the wet-chemistry CFA data, especially for Na.

smallest resolvable wavelength of the complete analytical setups, we use the intersection of bi-linear fits to the log-power spectral density of the raw, unfiltered data from the same section of data, shown in Figure 4[22].

With the 2.8 cm min^{-1} melt rate used for this run, the wavelengths indicated in Figure 4 translate to a resolution of 9.4 and 12.2 mm for the CFA Ca^{2+} and Na^{+} and 8.4 and 10.2 mm for the corresponding ICP data. The resolution differences between the ICP and the spectrophotometric methods arise due to the fact that both wet-chemistry methods use long mixing coils and in the case of Na^{+} a packed bead reactor, leading to signal dispersion that results in smoothing and tailing of peaks. Furthermore, the high resolution of the ICP data demonstrates the efficiency of its coupling to the melt-head with the use of segmented air/water flow and the small volume debubbler. Overall, the data of CFA-icpTOF has a higher resolution as the wet-chemistry CFA data. This is particularly evident in the comparison of the Na data sets, where the CFA-icpTOF resolves a lot more structure in the annual layer signal than the wet-chemistry CFA. This is especially important because the seasonal cycle in the concentration of sea-salt-derived sodium in the ice is an important marker for annual layer-counted time scales e.g.[23,24]. The higher resolution of the CFA-icpTOF data will enable the identification of annual layers further back in time, even if they are thinned by glacial flow.

It is worth noting, that the CFA-icpTOF measures the total elemental concentration in the ice whereas both spectrophotometric methods measure the dissolved fraction. That means the CFA-icpTOF will inadvertently measure higher concentrations if a non-negligible amount of undissolved mineral particles are present in the ice. In the case of the data presented here, the dust content of the ice is relatively low and hence no significant contribution of undissolved Ca or Na is expected. However, for ice from glacial periods or samples from locations with more proximal or stronger dust sources, the contribution from mineral dust will be higher due to the much higher dust concentrations and will likely lead to stronger deviations between the different detection methods

Single particle data

Using the high-resolution data acquired at 2 ms integration time and applying the detection algorithm described above, the data for each element can be decomposed into a signal attributed to particle ionization and the remainder. In the following we will refer to this remainder as the dissolved background signal, even though it results from both dissolved species as well as from particles below the lower particle detection limit. In this section we first focus on the decomposition of single-particle data for a single element, Fe, before we will expand the analysis to multi-elemental detection and fingerprinting of Fe-bearing particles, taking advantage of the detection capabilities of the TOFMS.

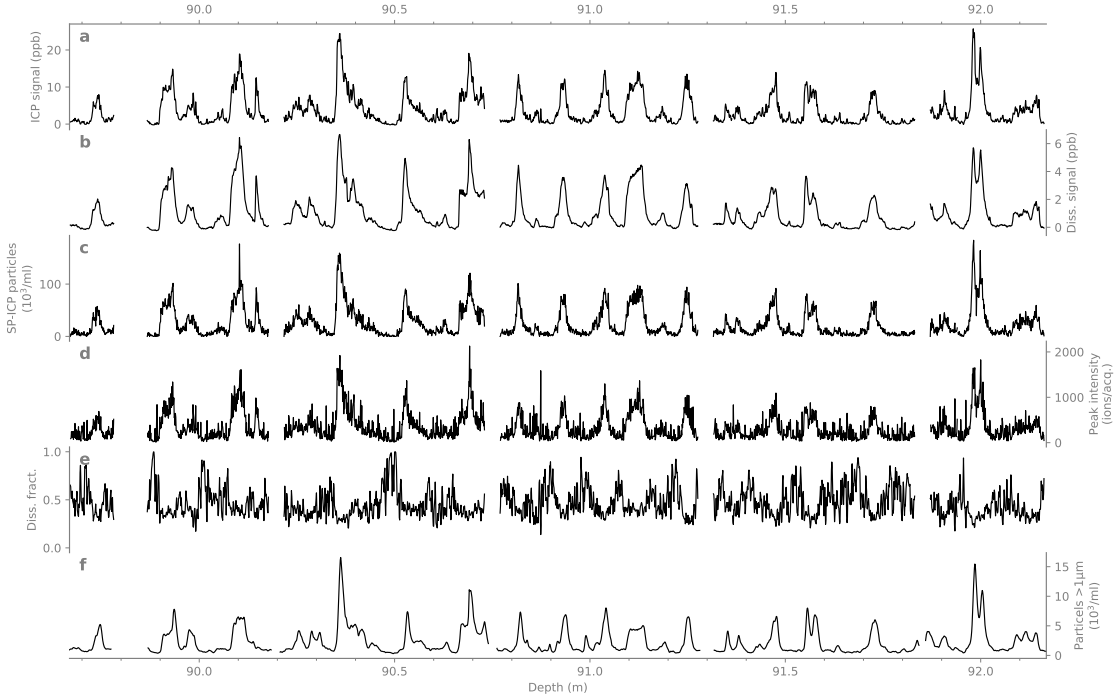

Figure 5: Decomposition of three meters of continuous Fe data into particulate and dissolved iron. From top to bottom, the panels show the total concentration signal (a), the dissolved concentration (b), the number of detected particles (c), the net amplitude of the detected particles signals (d), the fraction of the total signal that is attributed to the dissolved background (e) and in the bottom most panel (f) the micro-particle concentration in the ice as as measured by the Abakus Laser Particle Counter (Klotz) in the Bern CFA system.

Figure 5 shows a three meter section of Fe data from the CFA-icpTOF with its decomposition into particulate and dissolved signals alongside micro-particle concentrations as

determined by a laser particle counter[4,5]. Note that of the icpTOF data in Figure 5, only the total and dissolved Fe and the Fe-bearing particle number concentrations are calibrated quantities. The average intensity of the detected Fe-bearing particles also shown in Figure 5 is an uncalibrated quantity that is affected by the Fe-content of the particles, their size or a combination thereof. All of the Fe signals, both dissolved and particulate show a strong seasonal signal with annual peaks coinciding with the annual micro-particle peaks. The overall high correlation between the Fe signals and the micro-particle concentration is in good agreement with the fact, that the Fe content in the ice is governed by the deposition of particulate mineral dust aerosol onto the ice sheet. Considering all detected Fe-bearing particles, only 27 % of the total Fe is part of the dissolved background indicating that the iron deposition to the ice sheet is dominated by particulates. Despite the working definition of soluble iron used here, this value is in good agreement with other comparisons of dedicated soluble Fe and total Fe measurements in ice core samples from both Antarctica and Greenland that report soluble fractions between 20 and 30 %[25,26].

Focusing on the particulate fraction of the iron in the ice, the question arises how much of the insoluble iron is in the form of pure iron minerals such as iron oxides or hydroxides and how much of it is part of more complex minerals such as clay minerals. To target clay mineral particles we apply the particle detection algorithm independently to the Mg and Al traces of the same section of ice core as shown in Figure 5. From a purely qualitative view, a little more than half of the detected Fe-bearing particles (53 %) are not associated with peaks in either Mg or Al. However summing up the Fe peak intensities for the Fe only particles and particles detected in Fe and either Mg or Al reveals that around 74 % of the total mass of Fe detected in particles is also associated with either Mg or Al. This suggests that in terms of mass, most of the particulate iron deposited on the Greenland ice sheet is likely associated with clay mineral particles. Clay minerals make up a large fraction of the insoluble dust in Greenland ice both in recent time as well as in the past underlining the notion that the iron-bearing aerosol concentration co-varies with the particulate atmospheric

dust concentration[27–29].

To further characterize these mixed particles we investigate their composition in terms of elemental ratios. To do that, we calculate Mg/Al and Fe/Al mass ratios from the peak intensities for peaks co-occurring in Fe, Mg and Al, taking into account the respective sensitivities as determined by the standard measurements. In the following, only particles with overall uncertainties of less than 20 % RSTD in both elemental ratios are considered to limit the influence of particles with very large uncertainties. The resulting mass ratios for the individual particles are shown in a two dimensional histogram in Figure 6. Using isotope ratios, the central Asian Taklamakan and Gobi deserts have previously been identified as the major source regions for mineral dust transported to Greenlande.g.[27,29,30]. The mass ratio of iron to aluminum in the particles is 1.13 (-0.94/+6.52) (median and 90 % confidence interval) in good agreement with bulk measurements of Asian dust samples from the Taklamakan and Gobi deserts ranging from 0.36 to 1.60 with no uncertainty estimates[31,32].

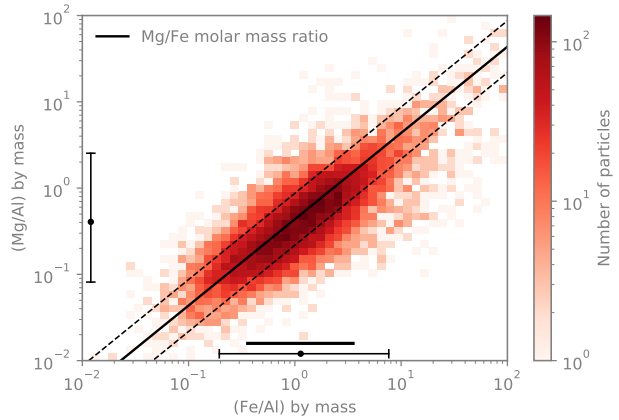

Figure 6: Histogram of Mg/Al and Fe/Al mass ratios of particles in all three elements in the section of data shown in Figure 5. The dots with error bars show the median and 90 % interval of the observed ratios whereas the thick solid line shows the range of values reported by[31] for Asian dust. The solid and dashed lines show the 1:1 and 2:1/1:2 atomic weight ratios of Mg/Fe.

Overall, the elemental ratios for the particles cluster around the Mg/Fe molar mass ratio line shown in Figure 6. This suggests, that the particles are consistent with a mineral that has a structure in which Mg and Fe atoms takes the same latice location and are interchangeable,

such as the clay mineral illite. Of the clay minerals found in Greenland ice, illite is by far the most abundant, contributing more than 50 % of the total amount of clay minerals in Greenland dust[27].

The addition of the icpTOF has extended the analytical capabilities of the Bern CFA system in two major ways. Firstly, it extends the analytes that can be measured in the ice to a wide range of elemental concentrations covering both mineral-dust and sea-salt sources. In comparison with the established methods, the resulting time series of total concentrations have at least similar and in some cases higher time resolution. This is especially important in the light of thinned ice core samples where the detection of annual layer signals is limited by the measurement techniques. Secondly, due to the fast sampling frequencies that are possible with a TOFMS, the setup is capable of resolving transient signals from the ionization of insoluble particles in the ice while still covering the complete mass range. Using this data, information about the characteristics of the mineral dust particles in the ice can be accessed. In the future these data will be used to characterize the composition and sources of insoluble particles in the ice both using a wider range of elements as well as targeting other types of particles such as tephra.

Acknowledgement

Purchase of the icpTOF has been made possible through the Swiss National Science Foundation (SNF) R'Equip proposal iceCP-TOF (grant no. 206021_170739). The long-term financial support of ice core research at the University of Bern by the Swiss National Science Foundation (grant no. 200020_172506 (iCEP) and 20FI21_164190 (EGRIP)) is gratefully acknowledged.

The authors also gratefully acknowledge the contributions of the countless people that facilitated and took part in both the ice-core drilling and processing as well as the CFA melting campaigns.

EGRIP is directed and organized by the Center of Ice and Climate at the Niels Bohr Institute. It is supported by funding agencies and institutions in Denmark (A. P. Møller Foundation, University of Copenhagen), USA (US National Science Foundation, Office of Polar Programs), Germany (Alfred Wegener Institute, Helmholtz Centre for Polar and Marine Research), Japan (National Institute of Polar Research and Artic Challenge for Sustainability), Norway (University of Bergen and Bergen Research Foundation), Switzerland (Swiss National Science Foundation), France (French Polar Institute Paul-Emile Victor, Institute for Geosciences and Environmental research) and China (Chinese Academy of Sciences and Beijing Normal University).

The authors further thank the reviewers for their usefull comments that helped to improve the manuscript.

References

(1) Fuhrer, K.; Neftel, A.; Anklin, M.; Maggi, V. Continuous measurements of hydrogen peroxide, formaldehyde, calcium and ammonium concentrations along the new grip ice core from summit, Central Greenland. *Atmospheric Environment* **1993**, *27*, 1873–1880.

(2) Sigg, A.; Fuhrer, K.; Anklin, M.; Staffelbach, T.; Zurmuehle, D. A continuous analysis technique for trace species in ice cores. *Environmental Science & Technology* **1994**, *28*, 204–209.

(3) Röthlisberger, R.; Bigler, M.; Hutterli, M. A.; Sommer, S.; Stauffer, B.; Junghans, H. G.; Wagenbach, D.; Staufer, B.; Junghans, H. G.; Wagenbach, D. Technique for continuous high-resolution analysis of trace substances in firn and ice cores. *Environmental Science & Technology* **2000**, *34*, 338–342.

(4) Kaufmann, P. R.; Federer, U.; Hutterli, M. A.; Bigler, M.; Schüpbach, S.; Ruth, U.; Schmitt, J.; Stocker, T. F. An Improved Continuous Flow Analysis System for High-

Resolution Field Measurements on Ice Cores. *Environmental Science & Technology* **2008**, *42*, 8044–8050.

(5) Ruth, U.; Wagenbach, D.; Steffensen, J. P.; Bigler, M. Continuous record of microparticle concentration and size distribution in the central Greenland NGRIP ice core during the last glacial period. *Journal of Geophysical Research* **2003**, *108*, 4098–5000.

(6) Fischer, H.; Schüpbach, S.; Gfeller, G.; Bigler, M.; Röthlisberger, R.; Erhardt, T.; Stocker, T. F.; Mulvaney, R.; Wolff, E. W. Millennial changes in North American wildfire and soil activity over the last glacial cycle. *Nature Geoscience* **2015**, *8*, 723–727.

(7) Schüpbach, S. et al. Greenland records of aerosol source and atmospheric lifetime changes from the Eemian to the Holocene. *Nature Communications* **2018**, *9*, 1–10.

(8) Erhardt, T.; Capron, E.; Rasmussen, S. O.; Schüpbach, S.; Bigler, M.; Adolphi, F.; Fischer, H. Decadal-scale progression of the onset of Dansgaard–Oeschger warming events. *Climate of the Past* **2019**, *15*, 811–825.

(9) McConnell, J. R.; Lamorey, G. W.; Lambert, S. W.; Taylor, K. C. Continuous Ice-Core Chemical Analyses Using Inductively Coupled Plasma Mass Spectrometry. *Environmental Science & Technology* **2002**, *36*, 7–11.

(10) Knüsel, S.; Piguet, D. E.; Schwikowski, M.; Gäggeler, H. W. Accuracy of Continuous Ice-Core Trace-Element Analysis by Inductively Coupled Plasma Sector Field Mass Spectrometry. *Environmental Science & Technology* **2003**, *37*, 2267–2273.

(11) McConnell, J. R.; Edwards, R. Coal burning leaves toxic heavy metal legacy in the Arctic. *Proceedings of the National Academy of Sciences of the United States of America* **2008**, *105*, 12140–12144.

(12) Borovinskaya, O.; Hattendorf, B.; Tanner, M.; Gschwind, S.; Günther, D. A prototype of a new inductively coupled plasma time-of-flight mass spectrometer providing temporally resolved, multi-element detection of short signals generated by single particles and droplets. *J. Anal. At. Spectrom.* **2013**, *28*, 226–233.

(13) Praetorius, A.; Gundlach-Graham, A.; Goldberg, E.; Fabienke, W.; Navratilova, J.; Gondikas, A.; Kaegi, R.; Günther, D.; Hofmann, T.; von der Kammer, F. Single-particle multi-element fingerprinting (spMEF) using inductively-coupled plasma time-of-flight mass spectrometry (ICP-TOFMS) to identify engineered nanoparticles against the elevated natural background in soils. *Environmental Science: Nano* **2017**, *4*, 307–314.

(14) Bigler, M.; Svensson, A.; Kettner, E.; Vallelonga, P.; Nielsen, M. E.; Steffensen, J. P. Optimization of High-Resolution Continuous Flow Analysis for Transient Climate Signals in Ice Cores. *Environmental Science & Technology* **2011**, *45*, 4483–4489.

(15) Flory, C. A.; Hansen, S. C.; Myerholtz, C. Mass selective notch filter with quadrupole excision fields. *Hewlett Packard Company, Palo Alto, California* **1997**, *US*.

(16) Hendriks, L.; Gundlach-Graham, A.; Hattendorf, B.; Günther, D. Characterization of a new ICP-TOFMS instrument with continuous and discrete introduction of solutions. *Journal of Analytical Atomic Spectrometry* **2017**, *00*, 1–14.

(17) Rhodes, R. H.; Baker, J. A.; Millet, M.-A.; Bertler, N. A. Experimental investigation of the effects of mineral dust on the reproducibility and accuracy of ice core trace element analyses. *Chemical Geology* **2011**, *286*, 207–221.

(18) Pace, H. E.; Rogers, N. J.; Jarolimek, C.; Coleman, V. A.; Higgins, C. P.; Ranville, J. F. Determining transport efficiency for the purpose of counting and sizing nanoparticles via single particle inductively coupled plasma mass spectrometry. *Analytical Chemistry* **2011**, *83*, 9361–9369.

(19) Ebdon, L.; Foulkes, M. E.; Hill, S. Direct atomic spectrometric analysis by slurry atomisation. Part 9. Fundamental studies of refractory samples. *Journal of Analytical Atomic Spectrometry* **1990**, *5*, 67–73.

(20) Ebdon, L.; Collier, A. Particle size effects on kaolin slurry analysis by inductively coupled plasma-atomic emission spectrometry. *Spectrochimica Acta Part B: Atomic Spectroscopy* **1988**, *43*, 355–369.

(21) Gundlach-Graham, A.; Hendriks, L.; Mehrabi, K.; Günther, D. Monte Carlo Simulation of Low-Count Signals in Time-of-Flight Mass Spectrometry and its Application to Single-Particle Detection. *Analytical Chemistry* **2018**, *90*, 11847–11855.

(22) Rasmussen, S. O.; Andersen, K. K.; Bigler, M.; Johnsen, S. J.; McCormack, T. Deconvolution-based resolution enhancement of chemical ice core records obtained by continuous flow analysis. *Journal of Geophysical Research* **2005**, *110*, 1–7.

(23) Andersen, K. K.; Ditlevsen, P. D.; Rasmussen, S. O.; Clausen, H. B.; Vinther, B. M.; Johnsen, S. J.; Steffensen, J. P. Retrieving a common accumulation record from Greenland ice cores for the past 1800 years. *Journal of Geophysical Research Atmospheres* **2006**, *111*, 1–12.

(24) Gfeller, G.; Fischer, H.; Bigler, M.; Schüpbach, S.; Leuenberger, D.; Mini, O. Representativeness and seasonality of major ion records derived from NEEM firn cores. *The Cryosphere* **2014**, *8*, 1855–1870.

(25) Traversi, R.; Barbante, C.; Gaspari, V.; Fattori, I.; Largiuni, O.; Magaldi, L.; Udisti, R. Aluminium and iron record for the last 28 kyr derived from the Antarctic EDC96 ice core using new CFA methods. *Annals of Glaciology* **2004**, *39*, 300–306.

(26) Burgay, F.; Erhardt, T.; Lunga, D. D.; Jensen, C. M.; Spolaor, A.; Vallelonga, P.; Fischer, H.; Barbante, C. Fe2+ in ice cores as a new potential proxy to detect past volcanic eruptions. *Science of The Total Environment* **2018**, *654*, 1110–1117.

(27) Svensson, A.; Biscaye, P. E.; Grousset, F. E. Characterization of late glacial continental dust in the Greenland Ice Core Project ice core. *Journal of Geophysical Research: Atmospheres* **2000**, *105*, 4637–4656.

(28) Biscaye, P. E.; Grousset, F. E.; Revel, M.; der Gaast, S.; Zielinski, G. A.; Vaars, A.; Kukla, G. Asian provenance of glacial dust (stage 2) in the Greenland Ice Sheet Project 2 Ice Core, Summit, Greenland. *Journal of Geophysical Research* **1997**, *102*, 26765–26781.

(29) Bory, A.; Biscaye, P. E.; Svensson, A.; Grousset, F. E. Seasonal variability in the origin of recent atmospheric mineral dust at NorthGRIP, Greenland. *Earth and Planetary Science Letters* **2002**, *196*, 123–134.

(30) Bory, A.; Biscaye, P. E.; Grousset, F. E. Two distinct seasonal Asian source regions for mineral dust deposited in Greenland (NorthGRIP). *Geophysical Research Letters* **2003**, *30*, 1167.

(31) Formenti, P.; Schütz, L.; Balkanski, Y.; Desboeufs, K.; Ebert, M.; Kandler, K.; Petzold, A.; Scheuvens, D.; Weinbruch, S.; Zhang, D. Recent progress in understanding physical and chemical properties of African and Asian mineral dust. *Atmospheric Chemistry and Physics* **2011**, *11*, 8231–8256.

(32) Jeong, G. Y. Bulk and single-particle mineralogy of Asian dust and a comparison with its source soils. *Journal of Geophysical Research* **2008**, *113*, 1–16.

Graphical TOC Entry

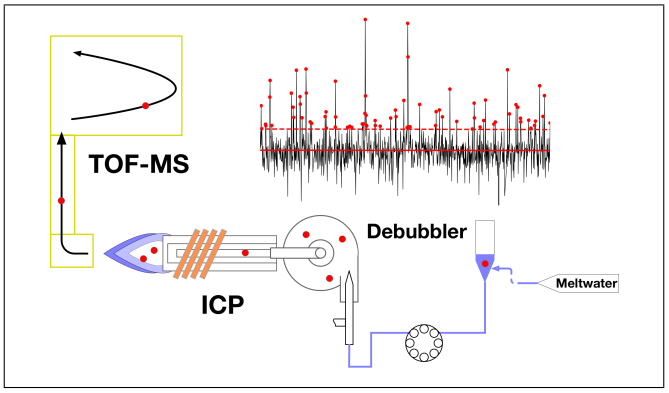

The graphical TOC shows a schematic representation of the sample introduction, ionization and detection of the single particle signals.